A Fixed-Point Iteration Scheme for Sensitivity-Based Distributed Optimal Control

Maximilian Pierer von Esch, Andreas Völz, and Knut Graichen, *Senior Member, IEEE*

***Abstract*—This article presents a sensitivity-based algorithm for distributed optimal control problems (OCP) of multi-agent systems with nonlinear dynamics and state/input couplings, as they arise, for instance, in distributed model predictive control. The algorithm relies on first-order sensitivities to cooperatively solve the distributed OCP in parallel. The solutions to the resulting local OCPs are computed with a fixed-point scheme and communicated within one communication step per algorithm iteration to the neighbors. Convergence results are presented under the inexact minimization of the local OCP. The algorithm is evaluated in numerical simulations for an example system.**

***Index Terms*—Agents and autonomous systems, distributed optimal control, nonlinear systems, optimization algorithms.**

I. Introduction

The problem of solving large-scale distributed optimal control problems (OCP) frequently arises in the context of distributed model predictive control (DMPC) for multi-agent systems [1], [2]. DMPC schemes offer the possibility of retaining the flexible, decentralized, and scalable structure of multi-agent systems while keeping the advantages of classical model predictive control, such as explicitly handling constraints and the applicability to nonlinear systems [3]. Besides iterative DMPC methods, there exist sequential schemes [4], robust methods in which couplings are viewed as disturbances [5], or methods imposing additional consistency constraints [6]. However, a large share of DMPC schemes employs iterative and cooperative methods where distributed OCPs are solved as they generally provide the best overall performance [2].

The idea is to solve the local OCP iteratively in parallel and exchange information on the respective solutions such that the local solutions converge toward the central problem. Prominent examples of algorithms used in such iterative schemes are the alternating direction method of multipliers (ADMM) [7], decentralized dual decomposition, or Jacobi iterations [8]. Another possibility is to apply sensitivity-based approaches where the local cost objectives are extended by linear approximations of the cost functional of neighboring subsystems mostly used in the context of linear systems [9], [10], [11]. However, extensions to nonlinear systems exist [12], [13], [14]. The main advantage of this approach is that, even for nonlinear OCPs, the sensitivities can be calculated in a computationally efficient manner using optimal control theory [12] and that only one neighbor-to-neighbor communication step per iteration is required [14]. Furthermore, numerical experiments have shown more favorable convergence properties compared to ADMM [14], [15].

This contribution presents a sensitivity-based approach first discussed in [12] and [14] to solve distributed OCPs with state/input couplings. Furthermore, the fixed-point scheme from [16] is applied to solve the local OCPs arising in the sensitivity-based approach in a computationally efficient manner. Although sufficient convergence conditions for the sensitivity-based approach have been derived for linear discrete-time systems [9] and algorithm variants considering the complete system dynamics on subsystem level [15], it still remains to investigate convergence properties for the general nonlinear continuous-time case in which only the local dynamics with state couplings are considered. This motivates extending the considerations of [9] and [15] to provide sufficient conditions for the convergence of the sensitivity-based algorithm [14] even with a finite number of fixed-point iterations since no convergence results are yet available [14]. In particular, it is shown that there exists an upper bound on the prediction horizon such that the proposed algorithm is convergent. If the scheme is used in a DMPC context, this constitutes a tradeoff between algorithm convergence, stability, and the performance of the DMPC scheme.

The rest of this article is organized as follows. In Section II, the central OCP is stated, for which the sensitivity-based distributed solution is shown in Section III. The convergence properties of the sensitivity-based algorithm and the fixed-point scheme are investigated for nonlinear continuous-time systems with pure state couplings. Afterward, the case of couplings in the controls is inspected. A numerical evaluation is conducted in Section IV. Finally, Section V concludes this article.

Several conventions are used in this text. The Euclidean norm of a vector $\boldsymbol{v} \in \mathbb{R}^v$ and the induced matrix norm of a matrix $\boldsymbol{M} \in \mathbb{R}^{m\times m}$ are denoted by $\|\boldsymbol{v}\|$ and $\|\boldsymbol{M}\|$, respectively. For a time (vector) function $\boldsymbol{v}(t) \in \mathbb{R}^v$, $t \in [0,T]$, the supremum norm $\|\boldsymbol{v}\|_{L_\infty} := \max_{[0,T]} \|\boldsymbol{v}(t)\|$ is used. An r-neighborhood of a point $\boldsymbol{v}_0 \in \mathbb{R}^v$ and a set $\mathcal{S} \subset \mathbb{R}^v$ are defined as $\mathcal{B}(\boldsymbol{v}_0, r) := \{\boldsymbol{v} \in \mathbb{R}^v \mid \|\boldsymbol{v} - \boldsymbol{v}_0\| \le r\}$ and $\mathcal{S}^r := \bigcup_{\boldsymbol{s}_0 \in \mathcal{S}} \mathcal{B}(\boldsymbol{s}_0, r)$, respectively. The stacking and reordering of vectors $\boldsymbol{v}_i \in \mathbb{R}^{v_i}$, $i \in \mathcal{V}$, from a set $\mathcal{V}$ is denoted as $\boldsymbol{v}_{\mathcal{V}}$. The partial derivative of a function $f(\boldsymbol{x},\boldsymbol{y})$ w.r.t. one of its arguments $\boldsymbol{x}$ is denoted as $\partial_{\boldsymbol{x}} f(\boldsymbol{x},\boldsymbol{y})$. For given iterates $(\boldsymbol{x}^k, \boldsymbol{y}^k)$ at step k of an algorithm, the notation $\partial_{\boldsymbol{x}} f^k = \partial_{\boldsymbol{x}} f(\boldsymbol{x},\boldsymbol{y})\big|_{\boldsymbol{x}=\boldsymbol{x}^k, \boldsymbol{y}=\boldsymbol{y}^k}$ is used. The explicit time dependency of trajectories, e.g., $\boldsymbol{v}(t)$, is omitted when convenient.

II. Problem Statement

Multi-agent systems are in general described by a graph $\mathcal{G} = (\mathcal{V}, \mathcal{E})$ with the set of vertices $\mathcal{V} = \{1,\dots,N\}$ and the set of edges $\mathcal{E} \subset \mathcal{V} \times \mathcal{V}$, which define the graph's adjacency matrix $\boldsymbol{A}$. The vertices $i \in \mathcal{V}$ are also referred to as agents and represent single dynamic subsystems. The set of edges defines the neighborhood $\mathcal{N}_i = \{j \in \mathcal{V} : (j,i) \in \mathcal{E}, j \neq i\}$ of agents directly coupled with agent $i \in \mathcal{V}$. The agent dynamics

Received 8 October 2024; accepted 12 November 2024. Date of publication 25 November 2024; date of current version 31 March 2025. This work was supported by the Deutsche Forschungsgemeinschaft (DFG, German Research Foundation) under Grant Gr 3870/6-1. Recommended by Associate Editor A. Astolfi. *(Corresponding author: Maximilian Pierer von Esch.)*

The authors are with the Chair of Automatic Control, Friedrich-Alexander-Universität Erlangen-Nürnberg (FAU), 91058 Erlangen, Germany (e-mail: maximilian.v.pierer@fau.de; andreas.voelz@fau.de; knut.graichen@fau.de).

Digital Object Identifier 10.1109/TAC.2024.3505753

are described by the nonlinear neighbor- and input-affine systems

$$\dot{\boldsymbol{x}}_i = \boldsymbol{f}_{ii}(\boldsymbol{x}_i) + \boldsymbol{B}_i(\boldsymbol{x}_i)\boldsymbol{u}_i + \sum_{j\in\mathcal{N}_i} \boldsymbol{f}_{ij}(\boldsymbol{x}_i,\boldsymbol{x}_j)\,, \quad \boldsymbol{x}_i(0)=\boldsymbol{x}_{i,0}$$
$$=: \boldsymbol{f}_i(\boldsymbol{x}_i,\boldsymbol{u}_i,\boldsymbol{x}_{\mathcal{N}_i})\,, \quad \boldsymbol{x}_i(0)=\boldsymbol{x}_{i,0} \tag{1}$$

with the state $\boldsymbol{x}_i \in \mathbb{R}^{n_i}$ and input $\boldsymbol{u}_i \in \mathbb{R}^{m_i}$ of agent $i \in \mathcal{V}$ as well as state $\boldsymbol{x}_j \in \mathbb{R}^{n_j}$ of neighbor $j \in \mathcal{N}_i$. It is assumed that the functions $\boldsymbol{f}_{ii} : \mathbb{R}^{n_i} \to \mathbb{R}^{n_i}$, $\boldsymbol{B}_i : \mathbb{R}^{n_i} \to \mathbb{R}^{n_i\times m_i}$, and $\boldsymbol{f}_{ij} : \mathbb{R}^{n_i} \times \mathbb{R}^{n_j} \to \mathbb{R}^{n_i}$ are continuously differentiable in their arguments. The input is subject to the (vector-valued) pointwise-in-time constraints $\boldsymbol{u}_i(t) \in [\boldsymbol{u}_i^-, \boldsymbol{u}_i^+]$, $t \in [0, T]$.

The central OCP to be solved in this article is of the form

$$\min_{\boldsymbol{u}_\mathcal{V}} \quad \sum_{i\in\mathcal{V}} J_i(\boldsymbol{x}_i,\boldsymbol{u}_i,\boldsymbol{x}_{\mathcal{N}_i}) \tag{2a}$$
$$\text{s.t} \quad \dot{\boldsymbol{x}}_i = \boldsymbol{f}_i(\boldsymbol{x}_i,\boldsymbol{u}_i,\boldsymbol{x}_{\mathcal{N}_i})\,, \quad \boldsymbol{x}_i(0) = \boldsymbol{x}_{i,0}\,, \quad i\in\mathcal{V} \tag{2b}$$
$$\boldsymbol{u}_i(t) \in [\boldsymbol{u}_i^-,\boldsymbol{u}_i^+]\,, \quad t\in[0,T], \quad i\in\mathcal{V} \tag{2c}$$

with the local cost functions (2a)

$$J_i(\boldsymbol{x}_i,\boldsymbol{u}_i,\boldsymbol{x}_{\mathcal{N}_i}) := V_i(\boldsymbol{x}_i(T)) + \int_0^T l_i(\boldsymbol{x}_i,\boldsymbol{u}_i,\boldsymbol{x}_{\mathcal{N}_i})\,\mathrm{d}t \tag{3}$$

and the time horizon $T > 0$. The integral cost function $l_i : \mathbb{R}^{n_i} \times \mathbb{R}^{m_i} \times \prod_{j\in\mathcal{N}_i} \mathbb{R}^{n_j} \to \mathbb{R}$ in (2a) is given by

$$l_i(\boldsymbol{x}_i,\boldsymbol{u}_i,\boldsymbol{x}_{\mathcal{N}_i}) := l_{ii}(\boldsymbol{x}_i) + \frac{1}{2}\bar{\boldsymbol{u}}_i^\top \boldsymbol{R}_i \bar{\boldsymbol{u}}_i + \sum_{j\in\mathcal{N}_i} l_{ij}(\boldsymbol{x}_i,\boldsymbol{x}_j) \tag{4}$$

with the quadratic term for the control $\bar{\boldsymbol{u}}_i := \boldsymbol{u}_i - \boldsymbol{u}_{i,\text{ref}}$ w.r.t. some reference $\boldsymbol{u}_{i,\text{ref}} \in \mathbb{R}^{m_i}$ and the diagonal positive-definite weighting matrix $\boldsymbol{R}_i \in \mathbb{R}^{m_i\times m_i}$. Moreover, the cost functions $l_{ii} : \mathbb{R}^{n_i} \to \mathbb{R}$, $l_{ij} : \mathbb{R}^{n_i} \times \mathbb{R}^{n_j} \to \mathbb{R}$, and $V_i : \mathbb{R}^{n_i} \to \mathbb{R}$ need to be continuously differentiable in their arguments.

III. Distributed Sensitivity-Based Solution

The main idea of the proposed algorithm is to solve the central OCP (2) in a distributed fashion while accounting for the couplings in the dynamics (1) and costs (4). This section presents the sensitivity-based algorithm as well as the fixed-point iteration scheme for the efficient solution of the local problems and investigates the overall convergence results.

A. Sensitivity-Based Algorithm

The general idea of the sensitivity-based distributed solution of the central OCP (2) is to extend the local cost (2a) of each agent by the first-order sensitivities of its neighbors [12]. The sensitivity represents the information about the expected change in the neighbor's cost w.r.t. the agent's own state and control trajectories. Augmenting (2a) with these sensitivities leads to the following OCP at iteration k for an agent $i \in \mathcal{V}$

$$\min_{\boldsymbol{u}_i} \quad \bar{J}_i(\boldsymbol{x}_i,\boldsymbol{u}_i,\boldsymbol{x}_{\mathcal{N}_i}^{k-1}) := J_i(\boldsymbol{x}_i,\boldsymbol{u}_i,\boldsymbol{x}_{\mathcal{N}_i}^{k-1})$$
$$+ \sum_{j\in\mathcal{N}_i} \delta\bar{J}_j(\boldsymbol{x}_j^{k-1},\boldsymbol{u}_j^{k-1},\boldsymbol{x}_{\mathcal{N}_j}^{k-1})(\delta\boldsymbol{x}_i) \tag{5a}$$
$$\text{s.t.} \quad \dot{\boldsymbol{x}}_i = \boldsymbol{f}_i(\boldsymbol{x}_i,\boldsymbol{u}_i,\boldsymbol{x}_{\mathcal{N}_i}^{k-1})\,, \quad \boldsymbol{x}_i(0) = \boldsymbol{x}_{i,0} \tag{5b}$$
$$\boldsymbol{u}_i(t) \in [\boldsymbol{u}_i^-,\boldsymbol{u}_i^+]\,, \quad t\in[0,T] \tag{5c}$$

with the neighbors' cost sensitivity represented by the corresponding Gâteaux derivative $\delta\bar{J}_j$ in direction of $\delta\boldsymbol{x}_i := \boldsymbol{x}_i - \boldsymbol{x}_i^{k-1}$ [14]. The dynamics (1) and cost terms (4) are decoupled by using the trajectories $\boldsymbol{x}_j^{k-1}$ of the previous iteration $k-1$, which need to be communicated by each agent.

The first-order optimality conditions for the local OCPs (5) consist of the canonical boundary value problem (BVP)

$$\dot{\boldsymbol{x}}_i = \boldsymbol{f}_i(\boldsymbol{x}_i,\boldsymbol{u}_i,\boldsymbol{x}_{\mathcal{N}_i}^{k-1})\,, \qquad \boldsymbol{x}_i(0) = \boldsymbol{x}_{i,0} \tag{6a}$$
$$\dot{\boldsymbol{\lambda}}_i = -\partial_{\boldsymbol{x}_i} H_i(\boldsymbol{x}_i,\boldsymbol{u}_i,\boldsymbol{\lambda}_i)\,, \qquad \boldsymbol{\lambda}_i(T) = \boldsymbol{\lambda}_{i,T} \tag{6b}$$

with the adjoint state $\boldsymbol{\lambda}_i \in \mathbb{R}^{n_i}$ and the terminal value $\boldsymbol{\lambda}_{i,T} := \partial_{\boldsymbol{x}_i} V_i(\boldsymbol{x}_i(T))$ and the minimization of the local Hamiltonian

$$H_i(\boldsymbol{x}_i,\boldsymbol{u}_i,\boldsymbol{\lambda}_i) := l_i(\boldsymbol{x}_i,\boldsymbol{u}_i,\boldsymbol{x}_{\mathcal{N}_i}^{k-1}) + \boldsymbol{\lambda}_i^\top \boldsymbol{f}_i(\boldsymbol{x}_i,\boldsymbol{u}_i,\boldsymbol{x}_{\mathcal{N}_i}^{k-1})$$
$$+ \sum_{j\in\mathcal{N}_i} \underbrace{(\partial_{\boldsymbol{x}_i} l_{ji}^{k-1} + (\partial_{\boldsymbol{x}_i} \boldsymbol{f}_{ji}^{k-1})^\top \boldsymbol{\lambda}_j^{k-1})^\top}_{=:\, \boldsymbol{g}_{ji}^{k-1}(t)} \delta\boldsymbol{x}_i\,. \tag{7}$$

w.r.t. the control, i.e.,

$$\min_{\boldsymbol{u}_i\in[\boldsymbol{u}_i^-,\boldsymbol{u}_i^+]} H_i(\boldsymbol{x}_i(t),\boldsymbol{u}_i,\boldsymbol{\lambda}_i(t))\,, \quad t\in[0,T]\,. \tag{8}$$

In (7), $\boldsymbol{\lambda}_j^{k-1}$ denotes the adjoint states of the neighbors $j \in \mathcal{N}_i$ from the previous iteration $k-1$, which also need to be communicated. In addition, the Gâteaux derivative $\delta\bar{J}_j$ in (5a) can be expressed as (see Appendix A for an explicit derivation)

$$\delta\bar{J}_j(\boldsymbol{x}_j^{k-1},\boldsymbol{u}_j^{k-1},\boldsymbol{x}_{\mathcal{N}_j}^{k-1})(\delta\boldsymbol{x}_i) = \int_0^T (\boldsymbol{g}_{ji}^{k-1})^\top \delta\boldsymbol{x}_i\,\mathrm{d}t, \tag{9}$$

where the gradients $\boldsymbol{g}_{ji}^{k-1}$ as defined in (7) involve the evaluation of partial derivatives in terms of the trajectories $\boldsymbol{x}_i^{k-1}(t)$, $\boldsymbol{x}_j^{k-1}(t)$, and $\boldsymbol{\lambda}_j^{k-1}(t)$, $t\in[0,T]$ and therefore are time trajectories themselves, i.e., $\boldsymbol{g}_{ji}^{k-1} = \boldsymbol{g}_{ji}^{k-1}(t)$. Moreover, no partial derivatives w.r.t. $\boldsymbol{u}_i$ appear in the definition of $\boldsymbol{g}_{ji}^{k-1}$ as only state couplings in the dynamics (1) and cost terms (4) are considered at this stage. Notice that the gradient $\boldsymbol{g}_{ji}^{k-1}$ can be calculated locally by each agent for its neighbors $j \in \mathcal{N}_i$ due to the neighbor-affine structure of (1) and (4) as long as the agent has access to the coupling functions l_{ji} and $\boldsymbol{f}_{ji}$.

In view of the preceding considerations, the steps for the sensitivity-based distributed OCP scheme are summarized in Algorithm 1. A convergence criterion is omitted for sake of simplicity. Note that Algorithm 1 relies on solving the optimality conditions (6) and (8) of OCP (5) in order to cooperatively arrive at the solution of OCP (2). Alternatively, a standard OCP solver can be used to compute $(\boldsymbol{u}_i^k, \boldsymbol{x}_i^k)$ in each iteration k, but then the adjoint dynamics (6b) must be solved backward in time to obtain $\boldsymbol{\lambda}_i^k$.

Remark 1: For nonneighbor-affine systems, such as $\boldsymbol{f}_i(\boldsymbol{x}_i,\boldsymbol{u}_i,\boldsymbol{x}_{\mathcal{N}_i}) = \boldsymbol{f}_{ii}(\boldsymbol{x}_i,\boldsymbol{x}_{\mathcal{N}_i}) + \boldsymbol{B}_i(\boldsymbol{x}_i)\boldsymbol{u}_i$, Algorithm 1 requires slight modifications. Specifically, the agents can no longer compute the sensitivities locally because (9) would potentially involve trajectories of second-order neighbors. As a result, an additional communication step must be introduced after Step 2 of Algorithm 1, in contrast to the single step in the current algorithm. However, we focus on the neighbor-affine form as it presents a compromise between covering a wide range of multi-agent systems and a reduced communication effort.

B. Local OCP Solution by Fixed-Point Iteration

In each iteration k of Algorithm 1, the optimality conditions (6) and (8) need to be solved in a computationally efficient manner. An elegant way is to follow the idea in [16] and to exploit the structure of (6) and (8) in a fixed-point iteration approach. Since the minimization problem (8) is strictly convex and separable in the single elements of

Algorithm 1: Distributed Sensitivity-Based Solution of OCP (2).

Initialize & send $\boldsymbol{u}_i^0(t)$, $\boldsymbol{x}_i^0(t)=\boldsymbol{x}_{i,0}$, $\boldsymbol{\lambda}_i^0(t)=\partial_{\boldsymbol{x}_i}V_i(\boldsymbol{x}_{i,0})$ to neighborhood $\mathcal{N}_i$, set $k \leftarrow 1$, and choose $k_{\max}$

1: **While** $k \leq k_{\max}$ **do**
2: Compute $\boldsymbol{g}_{ji}^{k-1}$ locally for all neighbors $j \in \mathcal{N}_i$
3: Compute $(\boldsymbol{u}_i^k, \boldsymbol{x}_i^k, \boldsymbol{\lambda}_i^k)$ locally by solving (6) and (8)
4: Send trajectories $(\boldsymbol{u}_i^k, \boldsymbol{x}_i^k, \boldsymbol{\lambda}_i^k)$ to all neighbors $j \in \mathcal{N}_i$
5: Set $k \leftarrow k+1$
6: **End While**

Algorithm 2: Solution of the Local OCP (5) in Step 3 of Algorithm 1 via Fixed-Point Iterations.

Initialize $\boldsymbol{\lambda}_i^{0|k} = \boldsymbol{\lambda}_i^{k-1}$, set $j \leftarrow 1$ and choose $j_{\max} =: r$

1: **While** $j \leq r$ **do**
2: Compute $\boldsymbol{x}_i^{j|k}(t)$ via forward integration of

$$\dot{\boldsymbol{x}}_i^{j|k} = \boldsymbol{F}_i(\boldsymbol{x}_i^{j|k}, \boldsymbol{\lambda}_i^{j-1|k}, \boldsymbol{x}_{\mathcal{N}_i}^{k-1}) \tag{13}$$

with initial condition $\boldsymbol{x}_i^{j|k}(0) = \boldsymbol{x}_{i,0}$
3: Compute $\boldsymbol{\lambda}_i^{j|k}(t)$ via backward integration of

$$\dot{\boldsymbol{\lambda}}_i^{j|k} = \boldsymbol{H}_i(\boldsymbol{x}_i^{j|k}, \boldsymbol{\lambda}_i^{j|k}, \boldsymbol{x}_i^{k-1}, \boldsymbol{x}_{\mathcal{N}_i}^{k-1}, \boldsymbol{\lambda}_{\mathcal{N}_i}^{k-1}) \tag{14}$$

with terminal condition $\boldsymbol{\lambda}_i^{j|k}(T) = \partial_{\boldsymbol{x}_i}V_i(\boldsymbol{x}_i^{j|k}(T))$
4: Set $j \leftarrow j+1$
5: **End While**
6: Compute $\boldsymbol{u}_i^k = \boldsymbol{h}_i(\boldsymbol{x}_i^{r|k}, \boldsymbol{\lambda}_i^{r|k})$, set $\boldsymbol{x}_i^k = \boldsymbol{x}_i^{r|k}$, $\boldsymbol{\lambda}_i^k = \boldsymbol{\lambda}_i^{r|k}$ and return to Step 4 of Algorithm 1

$\boldsymbol{u}_i$, the optimal control can be computed by the elementwise projection

$$u_{q,i} = h_{q,i}(\boldsymbol{x}_i, \boldsymbol{\lambda}_i) := \begin{cases} u_{q,i}^-, & \text{if } \hat{u}_{q,i} \leq u_{q,i}^- \\ u_{q,i}^+, & \text{if } \hat{u}_{q,i} \geq u_{q,i}^+ \\ \hat{u}_{q,i}, & \text{if } \hat{u}_{q,i} \in (u_{q,i}^-, u_{q,i}^+) \end{cases} \tag{10}$$

for each $u_{q,i}$ in $\boldsymbol{u}_i$ with $q \in \{1,\ldots,m_i\}$, $\boldsymbol{u}_i = \boldsymbol{h}_i(\boldsymbol{x}_i, \boldsymbol{\lambda}_i)$, and $\boldsymbol{h}_i = [h_{1,i},\ldots,h_{m_i,i}]^\top$. The unconstrained minimizer

$$\hat{u}_{q,i} = u_{q,i,\text{ref}} - r_{q,i}^{-1}\boldsymbol{b}_{q,i}^\top(\boldsymbol{x}_i)\boldsymbol{\lambda}_i \tag{11}$$

is obtained for each $u_{q,i,\text{ref}}$ in $\boldsymbol{u}_{i,\text{ref}}$, where $r_{q,i}$ is the qth diagonal element of $\boldsymbol{R}_i$, and $\boldsymbol{b}_{q,i}$ is the qth column of $\boldsymbol{B}_i$. Note that (10) is Lipschitz continuous but not differentiable [16] and only depends on $\boldsymbol{x}_i$ and $\boldsymbol{\lambda}_i$ due to the structure of the dynamics (1) and costs (4). Inserting (10) into the BVP (6) yields

$$\dot{\boldsymbol{x}}_i = \boldsymbol{F}_i(\boldsymbol{x}_i, \boldsymbol{\lambda}_i, \boldsymbol{x}_{\mathcal{N}_i}^{k-1}), \qquad \boldsymbol{x}_i(0) = \boldsymbol{x}_{i,0} \tag{12a}$$

$$\dot{\boldsymbol{\lambda}}_i = \boldsymbol{H}_i(\boldsymbol{x}_i, \boldsymbol{\lambda}_i, \boldsymbol{x}_i^{k-1}, \boldsymbol{x}_{\mathcal{N}_i}^{k-1}, \boldsymbol{\lambda}_{\mathcal{N}_i}^{k-1}), \qquad \boldsymbol{\lambda}_i(T) = \boldsymbol{\lambda}_{i,T} \tag{12b}$$

with the modified local functions $\boldsymbol{F}_i(\boldsymbol{x}_i, \boldsymbol{\lambda}_i, \boldsymbol{x}_{\mathcal{N}_i}^{k-1}) := \boldsymbol{f}_i(\boldsymbol{x}_i, \boldsymbol{h}_i(\boldsymbol{x}_i, \boldsymbol{\lambda}_i), \boldsymbol{x}_{\mathcal{N}_i}^{k-1})$ and $\boldsymbol{H}_i(\boldsymbol{x}_i, \boldsymbol{\lambda}_i, \boldsymbol{x}_i^{k-1}, \boldsymbol{x}_{\mathcal{N}_i}^{k-1}, \boldsymbol{\lambda}_{\mathcal{N}_i}^{k-1}) := -\partial_{\boldsymbol{x}_i}H_i(\boldsymbol{x}_i, \boldsymbol{h}_i(\boldsymbol{x}_i, \boldsymbol{\lambda}_i), \boldsymbol{\lambda}_i)$ by slight abuse of notations. The dependencies on external trajectories of neighbors in the previous iteration are now explicitly captured in $\boldsymbol{F}_i$ and $\boldsymbol{H}_i$.

The BVP (12) is efficiently solved by the local fixed-point iteration scheme illustrated in Algorithm 2. During the execution of Algorithm 1, the fixed-point iteration scheme is applied r times to solve the optimality conditions of the local OCP (5) before the calculated trajectories are communicated to the respective neighbors in Step 4 of Algorithm 1, i.e., $\boldsymbol{x}_i^k := \boldsymbol{x}_i^{r|k}$ and $\boldsymbol{\lambda}_i^k := \boldsymbol{\lambda}_i^{r|k}$. In the next optimization step $k+1$, Algorithm 2 is reinitialized with $\boldsymbol{\lambda}_i^{0|k+1} = \boldsymbol{\lambda}_i^k$.

Remark 2: For noninput-affine systems, the analytical computation of (10) is not possible, and a general approach to minimize (7), e.g., with the projected gradient method [17], is necessary, complicating the convergence analysis.

C. Convergence Properties of the Fixed-Point Iteration Scheme

In the following, the convergence of Algorithm 2 is examined as a prerequisite for subsequently investigating the overall convergence of Algorithm 1. Results in [16] show that the horizon length T is crucial for the convergence of the fixed-point iterations. A similar result is obtained in Theorem 1.

Theorem 1: There exists an upper bound $\bar{T} > 0$ such that for any $T < \bar{T}$, Algorithm 2 is contracting, i.e., there exists a $p \in (0,1)$ such that for all k

$$\|\Delta\boldsymbol{x}_i^{j|k}\|_{L_\infty} \leq p\|\Delta\boldsymbol{x}_i^{j-1|k}\|_{L_\infty}, \quad j = 2,3,\ldots \tag{15a}$$

$$\|\Delta\boldsymbol{\lambda}_i^{j|k}\|_{L_\infty} \leq p\|\Delta\boldsymbol{\lambda}_i^{j-1|k}\|_{L_\infty}, \quad j = 1,2,\ldots \tag{15b}$$

with $\Delta\boldsymbol{x}_i^{j|k} := \boldsymbol{x}_i^{j|k} - \boldsymbol{x}_i^{j-1|k}$ and $\Delta\boldsymbol{\lambda}_i^{j|k} := \boldsymbol{\lambda}_i^{j|k} - \boldsymbol{\lambda}_i^{j-1|k}$.

Proof: The following considerations require several Lipschitz estimates. Based on the continuous differentiability of dynamics and cost functions, there exist (local) Lipschitz constants $L_{F_i}, L_{H_i}, L_{V_i} > 0$ for some $r_{i,x}, r_{i,\lambda} > 0$ such that

$$\begin{aligned} &\|\boldsymbol{F}_i(\boldsymbol{x}_i, \boldsymbol{\lambda}_i, \boldsymbol{x}_{\mathcal{N}_i}) - \boldsymbol{F}_i(\boldsymbol{y}_i, \boldsymbol{\mu}_i, \boldsymbol{y}_{\mathcal{N}_i})\| \\ &\leq L_{F_i}\left(\|\boldsymbol{x}_i - \boldsymbol{y}_i\| + \|\boldsymbol{\lambda}_i - \boldsymbol{\mu}_i\| + \sum_{j\in\mathcal{N}_i}\|\boldsymbol{x}_j - \boldsymbol{y}_j\|\right) \end{aligned} \tag{16}$$

$$\begin{aligned} &\|\boldsymbol{H}_i(\boldsymbol{x}_i, \boldsymbol{\lambda}_i, \boldsymbol{x}_i, \boldsymbol{x}_{\mathcal{N}_i}, \boldsymbol{\lambda}_{\mathcal{N}_i}) - \boldsymbol{H}_i(\boldsymbol{y}_i, \boldsymbol{\mu}_i, \boldsymbol{y}_i, \boldsymbol{y}_{\mathcal{N}_i}, \boldsymbol{\mu}_{\mathcal{N}_i})\| \\ &\leq L_{H_i}\left(2\|\boldsymbol{x}_i - \boldsymbol{y}_i\| + \|\boldsymbol{\lambda}_i - \boldsymbol{\mu}_i\| + \sum_{j\in\mathcal{N}_i}(\|\boldsymbol{x}_j - \boldsymbol{y}_j\| + \|\boldsymbol{\lambda}_j - \boldsymbol{\mu}_j\|)\right) \end{aligned} \tag{17}$$

$$\|\partial_{\boldsymbol{x}_i}V_i(\boldsymbol{x}_i) - \partial_{\boldsymbol{x}_i}V_i(\boldsymbol{y}_i)\| \leq L_{V_i}\|\boldsymbol{x}_i - \boldsymbol{y}_i\| \tag{18}$$

for all $\boldsymbol{x}_i, \boldsymbol{y}_i \in \mathcal{B}_{i,x} := \mathcal{B}(\boldsymbol{x}_{i,0}, r_{i,x})$ and $\boldsymbol{\lambda}_i, \boldsymbol{\mu}_i \in \mathcal{S}_i^{r_{i,\lambda}}$, where $\mathcal{S}_i^{r_{i,\lambda}}$ is the $r_{i,\lambda}$-neighborhood to the compact set $\mathcal{S}_i := \{\partial_{\boldsymbol{x}_i}V_i(\boldsymbol{x}_i) \,|\, \boldsymbol{x}_i \in \mathcal{B}_{i,x}\}$. To ease the notation, we use the upper bounds $L_F = \max_{i\in\mathcal{V}}\{L_{F_i}\}$, $L_H = \max_{i\in\mathcal{V}}\{L_{H_i}\}$, and $L_V = \max_{i\in\mathcal{V}}\{L_{V_i}\}$ in the following.

At first, it is shown by induction that the iterates are bounded in each iteration k of Algorithm 1 for a sufficiently short time horizon T, i.e., $\boldsymbol{x}_i^{j|k}(t) \in \mathcal{B}_{i,x}$ and $\boldsymbol{\lambda}_i^{j|k}(t) \in \mathcal{S}_i^{r_{i,\lambda}}$, $t \in [0,T]$, for $j = 1,2,\ldots,r$. To this end, assume that $\boldsymbol{\lambda}_i^{j-1|k}(t) \in \mathcal{S}_i^{r_{i,\lambda}}$, $\boldsymbol{\lambda}_{\mathcal{N}_i}^{k-1}(t) \in \mathcal{S}_i^{r_{i,\lambda}}$, $\boldsymbol{x}_j^{k-1}(t) \in \mathcal{B}_{i,x}$, $j \in \mathcal{N}_i \cup i$, $t \in [0,T]$, and consider the integral form of (13). By adding and subtracting $\boldsymbol{F}_i(\boldsymbol{x}_{i,0}, \boldsymbol{\lambda}_{i,T}^{j-1|k}, \boldsymbol{x}_{\mathcal{N}_i,0})$ as well as using the Lipschitz property (16) and Gronwall's inequality [16], we get

$$\begin{aligned} \|\boldsymbol{x}_i^{j|k}(t) - \boldsymbol{x}_{i,0}\| &\leq \int_0^t \|\boldsymbol{F}_i(\boldsymbol{x}_i^{j|k}(\tau), \boldsymbol{\lambda}_i^{j-1|k}(\tau), \boldsymbol{x}_j^{k-1}(\tau))\|\,\mathrm{d}\tau \\ &\leq \mathrm{e}^{L_F t}\int_0^t L_F\left(\|\boldsymbol{\lambda}_i^{j-1|k} - \boldsymbol{\lambda}_{i,T}^{j-1|k}\| + \sum_{j\in\mathcal{N}_i}\|\boldsymbol{x}_j^{k-1} - \boldsymbol{x}_{j,0}\|\right) + h_{F_i}\,\mathrm{d}\tau \\ &\leq t\mathrm{e}^{L_F t}\left(L_F\left(r_{i,\lambda} + \sum_{j\in\mathcal{N}_i} r_{j,x}\right) + h_{F_i}\right) \end{aligned} \tag{19}$$

with the constant $h_{F_i} > 0$ and $\|\boldsymbol{F}_i(\boldsymbol{x}_{i,0}, \boldsymbol{\lambda}_{i,T}^{j-1|k}, \boldsymbol{x}_{\mathcal{N}_i,0})\| \leq h_{F_i}$. Thus, by choosing $T < T_x = \min_{i\in\mathcal{V}}\{T_{x_i}\}$ with T_{x_i} satisfying $T_{x_i}\mathrm{e}^{L_F T_{x_i}}(L_F(r_{i,\lambda} + \sum_{j\in\mathcal{N}_i} r_{j,x}) + h_{F_i}) = r_{i,x}$, the state trajectories are bounded, i.e., $\boldsymbol{x}_i^{j|k}(t) \in \mathcal{B}_{i,x}$, $t \in [0, T]$.

Similarly, consider the integral form of (14) in reverse time and the notation $\hat{y}(\tau) = y(T_x - \tau)$ for some trajectory $y(\tau)$, $\tau \in [0, T_x]$. By adding and subtracting $\boldsymbol{H}_i(\boldsymbol{x}_{i,0}, \boldsymbol{\lambda}_{i,T}^{j|k}, \boldsymbol{x}_{i,0}, \boldsymbol{x}_{\mathcal{N}_i,0}, \boldsymbol{\lambda}_{\mathcal{N}_i,T}^{k-1})$ as well as utilizing the Lipschitz property ((17)), Gronwall's inequality, and the fact that $\boldsymbol{x}_i^{j|k}(t) \in \mathcal{B}_{i,x}$, one gets (omitting time arguments)

$$\|\hat{\boldsymbol{\lambda}}_i^{j|k}(t) - \hat{\boldsymbol{\lambda}}_i^{j|k}(0)\| \leq \int_0^t \|\boldsymbol{H}_i(\hat{\boldsymbol{x}}_i^{j|k}, \hat{\boldsymbol{\lambda}}_i^{j|k}, \hat{\boldsymbol{x}}_i^{k-1}, \hat{\boldsymbol{x}}_{\mathcal{N}_i}^{k-1}, \hat{\boldsymbol{\lambda}}_{\mathcal{N}_i}^{k-1})\| \,\mathrm{d}\tau$$

$$\leq t\mathrm{e}^{L_H t}\left(L_H\left(2r_{i,x} + \sum_{j\in\mathcal{N}_i}(r_{j,x} + r_{j,\lambda})\right) + h_{H_i}\right) \tag{20}$$

with $\|\boldsymbol{H}_i(\boldsymbol{x}_{i,0}, \boldsymbol{\lambda}_{i,T}^{j|k}, \boldsymbol{x}_{i,0}, \boldsymbol{x}_{\mathcal{N}_i,0}, \boldsymbol{\lambda}_{\mathcal{N}_i,T}^{k-1})\| \leq h_{H_i}$. Thus, by choosing $T < \min\{T_x, T_\lambda\}$ with $T_\lambda = \min_{i\in\mathcal{V}}\{T_{\lambda_i}\} > 0$ satisfying $T_{\lambda_i}\mathrm{e}^{L_H T_{\lambda_i}}(L_H(2r_{i,x} + \sum_{j\in\mathcal{N}_i}(r_{j,x} + r_{j,\lambda}) + h_{H_i}) = r_{i,\lambda}$, the adjoint state trajectory is bounded, i.e., $\boldsymbol{\lambda}_i^{j|k}(t) \in \mathcal{S}_i^{r_{i,\lambda}}$ for $t \in [0, T_\lambda)$. Furthermore, note that $\boldsymbol{\lambda}_i^{0|0} = \boldsymbol{\lambda}_i^0(t) = \partial_{\boldsymbol{x}_i} V_i(\boldsymbol{x}_{i,0}) \in \mathcal{S}_i^{r_{i,\lambda}}$ and $\boldsymbol{x}_i^0(t) = \boldsymbol{x}_{i,0} \in \mathcal{B}_{i,x}$ $\forall i \in \mathcal{V}$ and that all $\boldsymbol{x}/\boldsymbol{\lambda}$-dependencies are passed on from previous iterations of Algorithm 2. This shows that for $T < \min\{T_x, T_\lambda\}$, all iterates stay within the respective sets $\mathcal{B}_{i,x}$ and $\mathcal{S}_i^{r_{i,\lambda}}$ are bounded and that existence of the integrals in steps (13) and (14) is ensured.

Next, the boundedness of the iterates is used to establish convergence of Algorithm 1. The proof follows the lines of [16, Lemma 1], which is adapted for the distributed OCP (5). Note that the external trajectories $\boldsymbol{x}_{\mathcal{N}_i}^{k-1}(t)$ and $\boldsymbol{\lambda}_{\mathcal{N}_i}^{k-1}(t)$ stay constant throughout the r local fixed-point iterations. Thus, based on the Lipschitz estimates (16) and (17), it can be shown that $\|\Delta\boldsymbol{x}_i^{j|k}\|_{L_\infty}$ and $\|\Delta\boldsymbol{\lambda}_i^{j|k}\|_{L_\infty}$ are bounded by [16]

$$\|\Delta\boldsymbol{x}_i^{j|k}\|_{L_\infty} \leq L_1\|\Delta\boldsymbol{\lambda}_i^{j-1|k}\|_{L_\infty} \tag{21a}$$

$$\|\Delta\boldsymbol{\lambda}_i^{j|k}\|_{L_\infty} \leq L_2\|\Delta\boldsymbol{x}_i^{j|k}\|_{L_\infty} \tag{21b}$$

with $L_1 = L_1(T) := L_F T\mathrm{e}^{L_F T}$ and $L_2 = L_2(T) := (L_V + L_H T)\mathrm{e}^{L_H T} > 0$. Inserting (21b) in (21a) and vice versa proves (1) with $p := L_1 L_2$. Thus, there exists a maximum horizon length $T_p := T_p(L_F, L_H, L_V)$ such that for all $T < T_p$, the contraction ratio satisfies $p < 1$. Combining the results shows that there exists a maximum horizon $\bar{T} := \min\{T_x, T_\lambda, T_p\}$ such that for $T < \bar{T}$, Algorithm 2 is contracting.

The results of Theorem 1 can be further strengthened under the assumption of convexity of the distributed OCP (5) or under the weaker assumption that its optimal solution is a unique stationary point. Then, Algorithm 2 implies the convergence to the optimal solution of OCP (5).

Remark 3: The explicit value of $\bar{T} = \min\{T_x, T_\lambda, T_p\}$ can be computed a priori with the Lambert W-function from the respective implicit relations for T_x, T_λ, and T_p found in the proof above. Typically, T_p is the limiting factor as the solution trajectories of (6) remain bounded for most physical systems.

Remark 4: If Algorithm 2 is used within an (D)MPC framework, the choice of T represents a tradeoff between the convergence of Algorithm 2 and the stability/performance of the DMPC scheme. This is related to the fact that a longer time horizon T typically leads to a larger domain of attraction. However, the upper bound on the time horizon can be enlarged by damping the iterates, which is discussed in the next section.

D. Convergence Properties of the Sensitivity-Based Algorithm

To investigate the convergence of the higher level sensitivity-based Algorithm 1, a measure of progression needs to be defined between two iterations k of Algorithm 1

$$\Delta\boldsymbol{x}_i^k := \boldsymbol{x}_i^{1|k+1} - \boldsymbol{x}_i^{r|k}, \quad \Delta\boldsymbol{\lambda}_i^k := \boldsymbol{\lambda}_i^{1|k+1} - \boldsymbol{\lambda}_i^{r|k} \tag{22}$$

which describes the difference between the solution after r fixed-point iterations at step k and the first fixed-point iteration at step $k+1$. Theorem 2 states the convergence condition of Algorithm 1 such that $\|\Delta\boldsymbol{x}_i^k\|_{L_\infty} \to 0$ and $\|\Delta\boldsymbol{\lambda}_i^k\|_{L_\infty} \to 0$, and shows that the limit point of Algorithm 1 fulfills the first-order optimality conditions of the central OCP (2). The stacking of the individual norms is described by $[\,\cdot\,]_{\mathcal{V}}$.

Theorem 2: There exists a maximum horizon length $0 < \hat{T} \leq \bar{T}$ with $\bar{T}$ according to Theorem 1 such that for any $T < \hat{T}$, Algorithm 1 is contracting, i.e., there exists an iteration matrix $\boldsymbol{P} \in \mathbb{R}^{2N\times 2N}$ such that

$$\begin{bmatrix}\|\Delta\boldsymbol{x}_i^k\|_{L_\infty}\\ \|\Delta\boldsymbol{\lambda}_i^k\|_{L_\infty}\end{bmatrix}_{\mathcal{V}} \leq \boldsymbol{P}\begin{bmatrix}\|\Delta\boldsymbol{x}_i^{k-1}\|_{L_\infty}\\ \|\Delta\boldsymbol{\lambda}_i^{k-1}\|_{L_\infty}\end{bmatrix}_{\mathcal{V}} \tag{23}$$

with $q := \|\boldsymbol{P}\| \in (0, 1)$. Moreover, the iterates $(\boldsymbol{x}_i^k, \boldsymbol{u}_i^k, \boldsymbol{\lambda}_i^k)$ are bounded and have limit points, which satisfy the first-order optimality conditions of the central problem (2).

Proof: Using (13) and $\boldsymbol{\lambda}_i^{0|k+1} = \boldsymbol{\lambda}_i^k$, the difference between the state trajectories $\boldsymbol{x}_i^{r|k}(t)$ and $\boldsymbol{x}_i^{1|k+1}(t)$ can be bounded under the Lipschitz property (16)

$$\|\boldsymbol{x}_i^{1|k+1}(t) - \boldsymbol{x}_i^{r|k}(t)\| = \|\Delta\boldsymbol{x}_i^k(t)\|$$

$$\leq \int_0^t \|\boldsymbol{F}_i(\boldsymbol{x}_i^{1|k+1}, \boldsymbol{\lambda}_i^{r|k}, \boldsymbol{x}_{\mathcal{N}_i}^{r|k}) - \boldsymbol{F}_i(\boldsymbol{x}_i^{r|k}, \boldsymbol{\lambda}_i^{r|k}, \boldsymbol{x}_{\mathcal{N}_i}^{r|k-1})\| \,\mathrm{d}\tau$$

$$\leq L_F \int_0^t \|\Delta\boldsymbol{x}_i^k(\tau)\| + \sum_{j\in\mathcal{N}_j}\|\boldsymbol{x}_j^{r|k}(\tau) - \boldsymbol{x}_j^{r|k-1}(\tau)\| \,\mathrm{d}\tau. \tag{24}$$

Applying Gronwall's inequality and the L_∞-norm on both sides shows that for all $i \in \mathcal{V}$

$$\|\Delta\boldsymbol{x}_i^k\|_{L_\infty} \leq L_1 \sum_{j\in\mathcal{N}_i}\|\boldsymbol{x}_j^{r|k} - \boldsymbol{x}_j^{r|k-1}\|_{L_\infty} \tag{25}$$

with the constant L_1 defined as before. Similarly, a bound on $\|\Delta\boldsymbol{\lambda}_i^k\|_{L_\infty}$ can be established by considering the integral form of (14) in reverse time at steps $r|k$ and $1|k+1$. A bound on $\|\Delta\boldsymbol{\lambda}_i^k\|$ follows from the Lipschitz estimate (17)

$$\|\hat{\boldsymbol{\lambda}}_i^{1|k+1}(t) - \hat{\boldsymbol{\lambda}}_i^{r|k}(t)\| = \|\Delta\hat{\boldsymbol{\lambda}}_i^k(t)\| \leq L_V\|\Delta\hat{\boldsymbol{x}}_i^k(0)\|$$

$$+ L_H \int_0^t \|\Delta\hat{\boldsymbol{x}}_i^k(\tau)\| + \|\Delta\hat{\boldsymbol{\lambda}}_i^k(\tau)\| + \|\hat{\boldsymbol{x}}_i^{r|k}(\tau) - \hat{\boldsymbol{x}}_i^{r|k-1}(\tau)\|$$

$$+ \sum_{j\in\mathcal{N}_i}\|\hat{\boldsymbol{x}}_j^{r|k}(\tau) - \hat{\boldsymbol{x}}_j^{r|k-1}(\tau)\| + \|\hat{\boldsymbol{\lambda}}_j^{r|k}(\tau) - \hat{\boldsymbol{\lambda}}_j^{r|k-1}(\tau)\| \,\mathrm{d}\tau. \tag{26}$$

Applying Gronwall's inequality and taking the L_∞-norm on both sides result in

$$\|\Delta\boldsymbol{\lambda}_i^k\|_{L_\infty} \leq L_2\|\Delta\boldsymbol{x}_i^k\|_{L_\infty} + L_3\|\boldsymbol{x}_i^{r|k} - \boldsymbol{x}_i^{r|k-1}\|_{L_\infty}$$

$$+ L_3 \sum_{j\in\mathcal{N}_i}\|\boldsymbol{x}_j^{r|k} - \boldsymbol{x}_j^{r|k-1}\|_{L_\infty} + \|\boldsymbol{\lambda}_j^{r|k} - \boldsymbol{\lambda}_j^{r|k-1}\|_{L_\infty} \tag{27}$$

with $L_3 = L_3(T) := L_H T\mathrm{e}^{L_H T} > 0$ and L_2 defined as before. The estimates $\|\boldsymbol{x}_j^{r|k} - \boldsymbol{x}_j^{r|k-1}\|_{L_\infty}$, $\|\boldsymbol{\lambda}_j^{r|k} - \boldsymbol{\lambda}_j^{r|k-1}\|_{L_\infty}$, and $\|\boldsymbol{x}_i^{r|k} - \boldsymbol{x}_i^{r|k-1}\|_{L_\infty}$ need to be formulated in terms of the bounds (22) such that (25) and (27) can be expressed in the form of (23). By adding and subtracting $\boldsymbol{x}_j^{1|k}$ and applying the triangle inequality, the norm $\|\boldsymbol{x}_j^{r|k} - \boldsymbol{x}_j^{r|k-1}\|_{L_\infty}$ can be expanded into two parts

$$\|\boldsymbol{x}_j^{r|k} - \boldsymbol{x}_j^{r|k-1}\|_{L_\infty} \leq \|\boldsymbol{x}_j^{r|k} - \boldsymbol{x}_j^{1|k}\|_{L_\infty} + \|\Delta\boldsymbol{x}_j^{k-1}\|_{L_\infty} \tag{28}$$

of which $\|\boldsymbol{x}_j^{r|k} - \boldsymbol{x}_j^{1|k}\|_{L_\infty}$ is further bounded by (52) in Appendix B

$$\|\boldsymbol{x}_j^{r|k} - \boldsymbol{x}_j^{1|k}\|_{L_\infty} \leq L_1 \frac{1-p^{r-1}}{1-p} \|\Delta\boldsymbol{\lambda}_j^{k-1}\|_{L_\infty} \tag{29}$$

resulting in the bound

$$\|\boldsymbol{x}_j^{r|k} - \boldsymbol{x}_j^{r|k-1}\|_{L_\infty} \leq \|\Delta\boldsymbol{x}_j^{k-1}\|_{L_\infty} + \alpha\|\Delta\boldsymbol{\lambda}_j^{k-1}\|_{L_\infty} \tag{30a}$$

with $\alpha := L_1 \frac{1-p^{r-1}}{1-p} > 0$. Following (28) and utilizing (53) in Appendix B, the bound

$$\|\boldsymbol{\lambda}_j^{r|k} - \boldsymbol{\lambda}_j^{r|k-1}\|_{L_\infty} \leq \beta\|\Delta\boldsymbol{\lambda}_j^{k-1}\|_{L_\infty} \tag{30b}$$

with $\beta := (1 + \frac{p-p^r}{1-p}) > 0$ is established in a similar fashion. Inserting (30a) and (30b) into (25) and (27) as well as concatenating all agents results in the linear discrete-time system (23) with

$$\boldsymbol{P} = \begin{bmatrix} L_1\boldsymbol{A} & \alpha L_1\boldsymbol{A} \\ L_3\boldsymbol{I} + \gamma\boldsymbol{A} & \alpha L_3\boldsymbol{I} + (\alpha\gamma + \beta L_3)\boldsymbol{A} \end{bmatrix} \tag{31}$$

$\gamma = \gamma(T) := (L_3 + L_1L_2) > 0$, and the adjacency matrix $\boldsymbol{A}$ of the graph $\mathcal{G}$. Clearly, $\boldsymbol{P}$ depends on the prediction horizon, i.e., $\boldsymbol{P}(T)$, and since $L_1(0) = L_3(0) = \gamma(0) = 0$, it follows that $\boldsymbol{P}(0) = \boldsymbol{0}$ implying $\|\boldsymbol{P}(0)\| = 0$. By continuity of $\|\boldsymbol{P}(T)\|$ w.r.t. T, there exists a maximum horizon length $\hat{T} := \hat{T}(L_F, L_H, L_V, p, r, \boldsymbol{A})$ such that for $T < \min\{\hat{T}, \bar{T}\}$, the linear discrete-time system in (23) is asymptotically stable with $\|\boldsymbol{P}\| \in (0,1)$.

The proof proceeds by showing that the limit point of the sequence $(\boldsymbol{x}_i^k,\ \boldsymbol{u}_i^k,\ \boldsymbol{\lambda}_i^k)$ satisfies the necessary first-order optimality conditions of the central problem (2). In Theorem 1, it was shown that $\boldsymbol{x}_i^k(t) \in \mathcal{B}_{i,x}$ as well as $\boldsymbol{\lambda}_i^k(t) \in \mathcal{S}_i^{r_{i,\lambda}}$, which implies that $\|\boldsymbol{x}_i^k(t)\| \leq M_x$ and $\|\boldsymbol{\lambda}_i^k(t)\| \leq M_\lambda\ \forall k,\ i \in \mathcal{V}$ and $t \in [0,\ T]$ for some constants $M_x,\ M_\lambda < \infty$ independent of k. In addition, according to (54) and (55) in Appendix B, asymptotic stability of (23) also implies $\|\boldsymbol{x}_i^{k+1} - \boldsymbol{x}_i^k\|_{L_\infty} \to 0$ and $\|\boldsymbol{\lambda}_i^{k+1} - \boldsymbol{\lambda}_i^k\|_{L_\infty} \to 0$ for $k \to \infty$. Thus, the sequence $(\boldsymbol{x}_i^k, \boldsymbol{\lambda}_i^k)$ is uniformly bounded on $[0, T]$ and has a bounded limit point $(\boldsymbol{x}_i^l,\ \boldsymbol{\lambda}_i^l)$. By the continuity of $\boldsymbol{h}_i$ in (10), the same is valid for the sequence $\boldsymbol{u}_i^k$ with limit point $\boldsymbol{u}_i^l$. The limit point then satisfies (13) and (14), i.e., $\dot{\boldsymbol{x}}_i^l = \boldsymbol{f}_i(\boldsymbol{x}_i^l, \boldsymbol{u}_i^l, \boldsymbol{x}_{\mathcal{N}_i}^l)$ and $\dot{\boldsymbol{\lambda}}_i^l = \partial_{\boldsymbol{x}_i} l_i^l + (\partial_{\boldsymbol{x}_i}\boldsymbol{f}_i^l)^\top\boldsymbol{\lambda}_i^l + \sum_{j\in\mathcal{N}_i} \partial_{\boldsymbol{x}_i} l_{ji}^l + (\partial_{\boldsymbol{x}_i}\boldsymbol{f}_{ji}^l)^\top\boldsymbol{\lambda}_j^l\ \forall i \in \mathcal{V}$. Utilizing the central Hamiltonian for OCP (2)

$$H(\boldsymbol{x}, \boldsymbol{u}, \boldsymbol{\lambda}) = \sum_{i\in\mathcal{V}} l_i(\boldsymbol{x}_i, \boldsymbol{u}_i, \boldsymbol{x}_{\mathcal{N}_i}) + \boldsymbol{\lambda}_i^\top \boldsymbol{f}_i(\boldsymbol{x}_i, \boldsymbol{u}_i, \boldsymbol{x}_{\mathcal{N}_i}) \tag{32}$$

with $\boldsymbol{x} := \boldsymbol{x}_\mathcal{V}$, $\boldsymbol{u} := \boldsymbol{u}_\mathcal{V}$, and $\boldsymbol{\lambda} := \boldsymbol{\lambda}_\mathcal{V}$, the central BVP reads

$$\dot{\boldsymbol{x}}_i = \boldsymbol{f}_i(\boldsymbol{x}_i, \boldsymbol{u}_i, \boldsymbol{x}_{\mathcal{N}_i}), \qquad \boldsymbol{x}_i(0) = \boldsymbol{x}_{i,0} \tag{33a}$$

$$\dot{\boldsymbol{\lambda}}_i = -\partial_{\boldsymbol{x}_i} H(\boldsymbol{x}, \boldsymbol{u}, \boldsymbol{\lambda}), \qquad \boldsymbol{\lambda}_i(T) = \boldsymbol{\lambda}_{i,T} \tag{33b}$$

for all $i \in \mathcal{V}$. Clearly, the dynamics of the limit point $\boldsymbol{x}_i^l$ equals the central dynamics (33a). To show that the adjoint state limit point $\boldsymbol{\lambda}_i^l$ fulfills the central adjoint dynamics, a closer look is taken at the right-hand side of (33b)

$$\partial_{\boldsymbol{x}_i} H(\boldsymbol{x}, \boldsymbol{u}, \boldsymbol{\lambda}) = \partial_{\boldsymbol{x}_i}\left(l_i + \boldsymbol{\lambda}_i^\top \boldsymbol{f}_i + \sum_{j\in\mathcal{N}_i} l_{ji} + \boldsymbol{\lambda}_j^\top \boldsymbol{f}_{ji} \right) \tag{34}$$

which corresponds to the right-hand side of the dynamics of the limit point of the adjoint state $\boldsymbol{\lambda}_i^l$ for all $i \in \mathcal{V}$, implying that (33b) and the dynamics of the limit point are identical. Furthermore, the minimizing control trajectory of the central problem is structurally identical to (10) as the minimization of the central Hamiltonian (32) is separable w.r.t $\boldsymbol{u}_i$ and thus leads to the same minimization problem (8) with solution $\boldsymbol{h}_i(\boldsymbol{x}_i, \boldsymbol{\lambda}_i)$. Thus, the limit points $(\boldsymbol{x}_i^l,\ \boldsymbol{u}_i^l,\ \boldsymbol{\lambda}_i^l)$ of the iterates fulfill the first-order optimality conditions of the central OCP (2). This proves Theorem 2.

In summary, Theorem 2 shows that explicit values for the prediction horizon can be computed a priori such that the sensitivity-based algorithm is linearly convergent. The bound $\hat{T}$ can be computed, for example, in a hierarchical fashion by a central entity, which assembles $\boldsymbol{P}$ and reduces T until $\|\boldsymbol{P}\| \leq 1$. To this end, it must receive local information, i.e., Lipschitz constants, from all agents and have knowledge of the graph structure. However, this value is usually quite conservative. Nevertheless, Theorem 2 states that a sufficiently small prediction horizon always exists such that Algorithm 1 converges even under the inexact minimization of the local OCPs (5) with Algorithm 2.

Remark 5: The iteration matrix $\boldsymbol{P}$ in (31) exhibits an interesting dependency on the adjacency matrix $\boldsymbol{A}$ in the sense that highly coupled systems with dense adjacency matrices exhibit a slower convergence rate than loosely coupled ones. This result reminds of the convergence properties for the classical consensus algorithm in which the convergence rate depends on the second-smallest eigenvalue of the graph Laplacian [18].

Remark 6: As mentioned above, the maximum horizon $\hat{T}$ can often be enlarged by damping the trajectories as proposed in [16] and [19], i.e., by performing

$$\boldsymbol{x}_i^{j|k}(t) \leftarrow (1-\epsilon)\boldsymbol{x}_i^{j|k}(t) + \epsilon\boldsymbol{x}_i^{k-1}(t), \quad t \in [0, T] \tag{35a}$$

$$\boldsymbol{\lambda}_i^{j|k}(t) \leftarrow (1-\epsilon)\boldsymbol{\lambda}_i^{j|k}(t) + \epsilon\boldsymbol{\lambda}_i^{k-1}(t), \quad t \in [0, T] \tag{35b}$$

as intermediate steps between Steps 2 and 3 or, respectively, between Steps 3 and 4 of Algorithm 2 with factor $\epsilon \in [0, 1)$.

Remark 7: Although the result of Theorem 2 again underpins the tradeoff between convergence and stability in the context of DMPC, this tradeoff is usually present regarding the numerical solution of OCPs in (D)MPC schemes. This is attributed to the fact that the computational burden is increased with a longer prediction horizon as usually more discretization points are necessary to accommodate the infinite-dimensional dynamic constraint (2b). This increased effort may jeopardize the stability of the (D)MPC scheme since a stabilizing solution might not be found anymore during the sampling time.

E. Extension to Input-State-Coupled Systems

This section considers the more general case in which the agent dynamics (1) are additionally influenced by the controls $\boldsymbol{u}_j \in \mathbb{R}^{m_j}$ of their respective neighbors, i.e.,

$$\dot{\boldsymbol{x}}_i = \boldsymbol{f}_i(\boldsymbol{x}_i, \boldsymbol{u}_i, \boldsymbol{x}_{\mathcal{N}_i}) + \sum_{j\in\mathcal{N}_i} \boldsymbol{B}_{ij}(\boldsymbol{x}_i)\boldsymbol{u}_j, \ \boldsymbol{x}_i(0) = \boldsymbol{x}_{i,0} \tag{36}$$

for all $i \in \mathcal{V}$ and $\boldsymbol{f}_i$ as defined in (1). It is assumed that the matrix function $\boldsymbol{B}_{ij} : \mathbb{R}^{n_i} \to \mathbb{R}^{n_i \times m_j}$ is continuously differentiable w.r.t. its arguments. The system description (36) represents a natural extension of input-affine systems to the neighbor-affine structure and appears for example in systems where agents share actuators or chemical reactors [20], [21]. The central OCP (2) stays the same besides replacing (2b) with (36). In the following, only the main differences to the state-coupled case are pointed out as the procedure of solving the local OCPs with Algorithm 2 and investigating convergence remains identical. The first major difference is that the unconstrained minimizer (11) is not only a function of local variables but also of external trajectories, i.e.,

$$\hat{u}_{q,i} = u_{q,i,\mathrm{ref}} - r_i^{-1}\left(\boldsymbol{b}_{q,i}^\top(\boldsymbol{x}_i)\boldsymbol{\lambda}_i + \sum_{j\in\mathcal{N}_i}\boldsymbol{b}_{s,ji}^\top(\boldsymbol{x}_j^{k-1})\boldsymbol{\lambda}_j^{k-1}\right) \tag{37}$$

with $\boldsymbol{b}_{s,ji}$ denoting the sth column of $\boldsymbol{B}_{ij}$, $s = 1,\ldots,m_j$, as the sensitivity w.r.t $\boldsymbol{u}_i$ is not zero, i.e., (9) becomes

$$\begin{aligned}&\delta J_j(\boldsymbol{x}_j^{k-1}, \boldsymbol{u}_j^{k-1}, \boldsymbol{x}_{\mathcal{N}_j}^{k-1}, \boldsymbol{u}_{\mathcal{N}_j}^{k-1})(\delta\boldsymbol{x}_i, \delta\boldsymbol{u}_i) = \\ &= \int_0^T (\boldsymbol{g}_{ji}^{k-1})^\top \delta\boldsymbol{x}_i + (\boldsymbol{\lambda}_j^{k-1})^\top \boldsymbol{B}_{ji}(\boldsymbol{x}_j^{k-1})\,\delta\boldsymbol{u}_i\,\mathrm{d}t\end{aligned} \tag{38}$$

compared to the case of pure state coupling (see Appendix A) with $\delta\boldsymbol{u}_i = \boldsymbol{u}_i - \boldsymbol{u}_i^{k-1}$. Thus, the minimizing control function in (10) also depends on previous (external) trajectories, i.e., $\boldsymbol{h}_i(\boldsymbol{x}_i, \boldsymbol{\lambda}_i, \boldsymbol{x}_{\mathcal{N}_i}^{k-1}, \boldsymbol{\lambda}_{\mathcal{N}_i}^{k-1})$. Inserting the new control into the BVP (12) results in

$$\dot{\boldsymbol{x}}_i = \boldsymbol{F}_i(\boldsymbol{x}_i, \boldsymbol{\lambda}_i, \boldsymbol{x}_{\mathcal{N}_i}^{k-1}, \boldsymbol{\lambda}_{\mathcal{N}_i}^{k-1}, \boldsymbol{x}_{\mathcal{N}_j}^{k-2}, \boldsymbol{\lambda}_{\mathcal{N}_j}^{k-2}) \tag{39a}$$

$$\dot{\boldsymbol{\lambda}}_i = \boldsymbol{H}_i(\boldsymbol{x}_i, \boldsymbol{\lambda}_i, \boldsymbol{x}_i^{k-1}, \boldsymbol{x}_{\mathcal{N}_i}^{k-1}, \boldsymbol{\lambda}_{\mathcal{N}_i}^{k-1}, \boldsymbol{x}_{\mathcal{N}_j}^{k-2}, \boldsymbol{\lambda}_{\mathcal{N}_j}^{k-2}) \tag{39b}$$

with initial condition $\boldsymbol{x}_i(0) = \boldsymbol{x}_{i,0}$ and terminal condition $\boldsymbol{\lambda}_i(T) = \boldsymbol{\lambda}_{i,T}$. Note that by inserting $\boldsymbol{u}_j^{k-1} = \boldsymbol{h}_j(\boldsymbol{x}_j, \boldsymbol{\lambda}_j, \boldsymbol{x}_{\mathcal{N}_j}^{k-1}, \boldsymbol{\lambda}_{\mathcal{N}_j}^{k-1})$ into (36) introduces trajectories with iteration index $k-2$. Moreover, the BVP (39) depends on the state and adjoint trajectories of the neighborhood $\mathcal{N}_j$ of each neighbor due to the input coupling. The next theorem investigates the error (22) throughout the iterations of Algorithm 1 with the modified BVP (39) instead of (12).

Theorem 3: There exists a maximum horizon length $0 < \hat{T} \le \bar{T}$ with $\bar{T}$ according to Theorem 1 such that for any $T < \hat{T}$, Algorithm 1 is contracting, i.e., there exist iteration matrices $\boldsymbol{P}_1, \boldsymbol{P}_2 \in \mathbb{R}^{2N\times 2N}$ such that

$$\begin{bmatrix}\|\Delta\boldsymbol{x}_i^k\|_{L_\infty}\\ \|\Delta\boldsymbol{\lambda}_i^k\|_{L_\infty}\end{bmatrix}_{\mathcal{V}} \le \boldsymbol{P}_1\begin{bmatrix}\|\Delta\boldsymbol{x}_i^{k-1}\|_{L_\infty}\\ \|\Delta\boldsymbol{\lambda}_i^{k-1}\|_{L_\infty}\end{bmatrix}_{\mathcal{V}} + \boldsymbol{P}_2\begin{bmatrix}\|\Delta\boldsymbol{x}_i^{k-2}\|_{L_\infty}\\ \|\Delta\boldsymbol{\lambda}_i^{k-2}\|_{L_\infty}\end{bmatrix}_{\mathcal{V}} \tag{40}$$

with $q := \|\boldsymbol{P}_1\| + \|\boldsymbol{P}_2\| \in (0,1)$. In addition, the iterates $(\boldsymbol{x}_i^k, \boldsymbol{u}_i^k, \boldsymbol{\lambda}_i^k)$ are bounded and have limit points, which satisfy the first-order optimality conditions of the central problem (2).

Proof: This proof closely resembles the proof of Theorem 2. Similar to (24)–(30), the following bounds on $\|\Delta\boldsymbol{x}_i^k\|_{L_\infty}$ and $\|\Delta\boldsymbol{\lambda}_i^k\|_{L_\infty}$ hold

$$\begin{aligned}\|\Delta\boldsymbol{x}_i^k\|_{L_\infty} \le{}& L_1\sum_{j\in\mathcal{N}_i}\|\Delta\boldsymbol{x}_j^{k-1}\|_{L_\infty} + (\alpha+\beta)\|\Delta\boldsymbol{\lambda}_j^{k-1}\|_{L_\infty}\\ &+ L_1\sum_{j\in\mathcal{N}_i}\sum_{s\in\mathcal{N}_j}\|\Delta\boldsymbol{x}_s^{k-2}\|_{L_\infty} + (\alpha+\beta)\|\Delta\boldsymbol{\lambda}_s^{k-2}\|_{L_\infty}\end{aligned} \tag{41}$$

$$\begin{aligned}\|\Delta\boldsymbol{\lambda}_i^k\|_{L_\infty} \le{}& L_2\|\Delta\boldsymbol{x}_i^k\|_{L_\infty} + L_3(\|\Delta\boldsymbol{x}_i^{k-1}\|_{L_\infty} + \alpha\|\boldsymbol{\lambda}_i^{k-1}\|_{L_\infty})\\ &+ L_3\sum_{j\in\mathcal{N}_i}\|\Delta\boldsymbol{x}_j^{k-1}\|_{L_\infty} + (\alpha+\beta)\|\Delta\boldsymbol{\lambda}_j^{k-1}\|_{L_\infty}\\ &+ L_3\sum_{j\in\mathcal{N}_i}\sum_{s\in\mathcal{N}_j}\|\Delta\boldsymbol{x}_s^{k-2}\|_{L_\infty} + (\alpha+\beta)\|\Delta\boldsymbol{\lambda}_s^{k-2}\|_{L_\infty}.\end{aligned} \tag{42}$$

Inserting (41) into (42) and concatenating all agents lead to (40) with the iteration matrices

$$\boldsymbol{P}_1 = \begin{bmatrix} L_1\boldsymbol{A} & L_1(\alpha+\beta)\boldsymbol{A}\\ L_3\boldsymbol{I} + \gamma\boldsymbol{A} & \alpha L_3\boldsymbol{I} + \gamma(\alpha+\beta)\boldsymbol{A}\end{bmatrix} \tag{43}$$

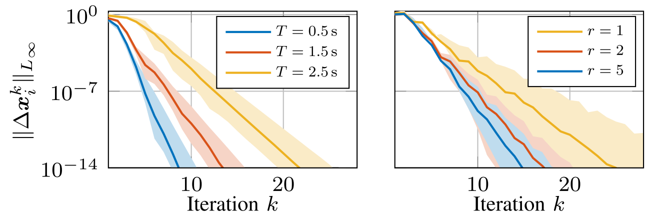

Fig. 1. Envelope over all sampled trajectories together with the median convergence curve of Algorithm 1 for random initial conditions and different time horizons T ($r = 2$, left) as well as different r ($T = 1.0\,\mathrm{s}$, right).

$$\boldsymbol{P}_2 = \begin{bmatrix} L_1\boldsymbol{A}^2 & L_1(\alpha+\beta)\boldsymbol{A}^2\\ \gamma\boldsymbol{A}^2 & \gamma(\alpha+\beta)\boldsymbol{A}^2\end{bmatrix}. \tag{44}$$

The asymptotic stability of (40) follows for $\|\boldsymbol{P}_1\| + \|\boldsymbol{P}_2\| < 1$, see [22, Th. 1]. Thus, a sufficiently short prediction horizon T can always be found as $\|\boldsymbol{P}_1\| \to 0$ and $\|\boldsymbol{P}_2\| \to 0$ for $T \to 0$. Similar to Theorem 2, it can be shown that the iterates are bounded and have limit points satisfying the first-order optimality conditions of the central problem (2).

The convergence condition $\|\boldsymbol{P}_1\| + \|\boldsymbol{P}_2\| < 1$ is clearly more restrictive in terms of the maximum allowable horizon length T than in the case where agents are only coupled in the states. This follows from the fact that input coupling introduces more dependencies on external trajectories in the BVP (39) compared to BVP (12). As in Section III-D, the horizon length can be enlarged by damping the iterates according to (35).

IV. Evaluation

The sensitivity-based algorithm is evaluated for a system of ten coupled Duffing oscillators [23]

$$\begin{bmatrix}\dot{x}_{1,i}\\ \dot{x}_{2,i}\end{bmatrix} = \begin{bmatrix} x_{2,i}\\ -\beta x_{1,i}^3 + x_{1,i}u_i + d\sum_{j\in\mathcal{N}_i} x_{1,i}x_{1,j}\end{bmatrix} \tag{45}$$

with $\beta = 1$ and coupling strength $d = 2$, which are arranged in a ring topology. The controls are constrained to the set $u_i \in [-1, 1]$. The quadratic integral cost functions $l_i(\boldsymbol{x}_i, u_i) = \frac{1}{2}(\boldsymbol{x}_i^\top\boldsymbol{Q}_i\boldsymbol{x}_i + R_i u_i^2)$ and terminal cost $V_i(\boldsymbol{x}_i) = 0$ are employed for all $i \in \mathcal{V}$ with the weighting matrices $\boldsymbol{Q}_i = \mathrm{diag}(1, 1)$ and $R_i = 1$, and a fourth-order Runge–Kutta scheme is used for the numerical integration of (13) and (14). Fig. 1 shows the evolution of the envelope and median norm $\|\Delta\boldsymbol{x}_i^k\|_{L_\infty}$ in the single iterations k of Algorithm 1 for 20 randomly sampled initial conditions $\boldsymbol{x}_{i,0} \in [0.75, 0.25] \times [0.75, 0.25]$. In the left plot of Fig. 1, the prediction horizon is varied while the fixed-point iterations are held constant at $r = 2$. As predicted by Theorem 2, a longer time horizon reduces the convergence speed. On the contrary, the horizon is held constant at $T = 1.0$ s and the number of fixed-point iterations is varied on the right-hand side of Fig. 1. Clearly, solving the local OCPs (5) to higher accuracy enhances the convergence rate as the bounds (30) become tighter. Theorem 2 furthermore indicates that the network topology influences the maximum horizon $\hat{T}$. To determine $\hat{T}$, the prediction horizon T is increased for different topologies until the algorithm diverges and the resulting curves w.r.t. the norm of the adjacency matrix $\|\boldsymbol{A}\|$ are depicted in Fig. 2. Hereby, the norm $\|\boldsymbol{A}\|$ acts as a measure of how interconnected the overall systems are. The maximum horizon $\hat{T}$ decreases exponentially for more densely coupled systems, but can be significantly enlarged by damping the iterates,

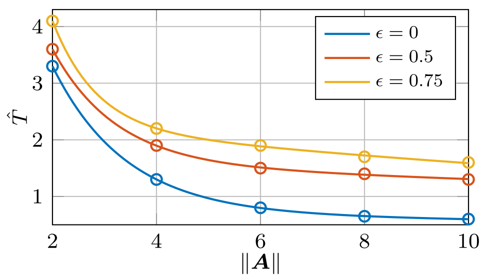

Fig. 2. Maximum time horizon $\hat{T}$ w.r.t. the norm of the adjacency matrix $\|\boldsymbol{A}\|$ as a measure of the coupling strength of the network topology and additional damping, with damping parameter ϵ (35), of the fixed-point iterations.

see (35). This is consistent with the results from [19] in the case of multi-agent systems.

V. Conclusion

This article presents the combination of a sensitivity-based algorithm and a fixed-point scheme to iteratively solve distributed OCPs with state or input coupling, as they arise, e.g., in DMPC. The combination is numerically efficient in the sense that the optimality conditions of the local OCP are solved within a coupled forward–backward integration and that the sensitivities can be calculated locally for each neighbor. This leads to a fully distributed algorithm with one communication step per algorithm iteration. Convergence is shown for an upper bound on the horizon length that can be seen as a tradeoff between convergence speed and stability of the sensitivity-based algorithm. In practice, however, the maximum horizon length can typically be enlarged by damping the iterates.

Future research will focus on investigating the convergence of an asynchronous version of the sensitivity-based algorithm in which agents can perform the local optimization with delayed trajectories. In addition, the presented distributed algorithm will be verified on distributed hardware setups.

Appendix A
Computation of Sensitivities

The idea of using sensitivities to modify cost functions goes back to the idea of partial goal-interaction operators [24]. We follow the spirit of the authors in [12], [13], and [14] and define this partial goal-interaction operator for the problem at hand. In general, the operator describes the influence that the variables of agent $i \in \mathcal{V}$ have on the central cost (2a) via the local cost of agent $j \in \mathcal{N}_i$.

In this regard, the interaction operator, i.e., the sensitivities, in the context of OCPs is defined as the Gâteaux derivative $\delta J_j(\boldsymbol{x}_j^k, \boldsymbol{u}_j^k, \boldsymbol{x}_{\mathcal{N}_j}^k)(\delta \boldsymbol{x}_i)$ of a single neighbor's OCP of the central formulation (2)

$$\min_{\boldsymbol{u}_j} \quad J_j(\boldsymbol{x}_j, \boldsymbol{u}_j, \boldsymbol{x}_{\mathcal{N}_j}) \tag{46a}$$

$$\text{s.t.} \quad \dot{\boldsymbol{x}}_j = \boldsymbol{f}_j(\boldsymbol{x}_j, \boldsymbol{u}_j, \boldsymbol{x}_{\mathcal{N}_j}), \quad \boldsymbol{x}_j(0) = \boldsymbol{x}_{j,0} \tag{46b}$$

$$\boldsymbol{u}_j(t) \in [\boldsymbol{u}_j^-, \boldsymbol{u}_j^+], \quad t \in [0, T] \tag{46c}$$

w.r.t. the admissible direction $\delta \boldsymbol{x}_i$ at some point $(\boldsymbol{x}_j^k, \boldsymbol{u}_j^k, \boldsymbol{x}_{\mathcal{N}_j}^k)$. The computation of the Gâteaux derivative is directly based on its definition

$$\delta J_j(\boldsymbol{x}_j^k, \boldsymbol{u}_j^k, \boldsymbol{x}_{\mathcal{N}_j}^k)(\delta \boldsymbol{x}_i) = \left.\frac{\mathrm{d} J_j(\boldsymbol{x}_j^k, \boldsymbol{u}_j^k, \boldsymbol{x}_{\mathcal{N}_j}^k + \epsilon\, \delta \bar{\boldsymbol{x}}_i)}{\mathrm{d}\epsilon}\right|_{\epsilon=0} \tag{47}$$

with the vector $\delta \bar{\boldsymbol{x}}_i = [\boldsymbol{0}^\top \ldots \boldsymbol{0}^\top\, \delta \boldsymbol{x}_i^\top\, \boldsymbol{0}^\top \ldots \boldsymbol{0}^\top]^\top \in \mathbb{R}^{p_j}$ with $p_j = \sum_{s \in \mathcal{N}_j} n_s$ and where $\delta \boldsymbol{x}_i$ shows up at the position corresponding to $\boldsymbol{x}_i$ in $\boldsymbol{x}_{\mathcal{N}_j}$.

Adjoining the dynamics to the cost via (time-dependent) Lagrange multipliers $\boldsymbol{\lambda}_j \in \mathbb{R}^{n_j}$, we get

$$\begin{aligned}
\delta J_j(\boldsymbol{x}_j^k, \boldsymbol{u}_j^k, \boldsymbol{x}_{\mathcal{N}_j}^k)(\delta \boldsymbol{x}_i) &= \int_0^T \frac{\mathrm{d}}{\mathrm{d}\epsilon} l_j(\boldsymbol{x}_j^k, \boldsymbol{u}_j^k, \boldsymbol{x}_{\mathcal{N}_j}^k + \epsilon \delta \bar{\boldsymbol{x}}_i) \\
&\quad + \frac{\mathrm{d}}{\mathrm{d}\epsilon}((\boldsymbol{\lambda}_j^k)^\top (\boldsymbol{f}_j(\boldsymbol{x}_j^k, \boldsymbol{u}_j^k, \boldsymbol{x}_{\mathcal{N}_j}^k + \epsilon \delta \bar{\boldsymbol{x}}_i) - \dot{\boldsymbol{x}}_j^k)\,\mathrm{d}t \bigg|_{\epsilon=0} \\
&= \int_0^T \partial_{\bar{\boldsymbol{x}}_i} \left(l_j(\boldsymbol{x}_j^k, \boldsymbol{u}_j^k, \boldsymbol{x}_{\mathcal{N}_j}^k) + (\boldsymbol{f}_j(\boldsymbol{x}_j^k, \boldsymbol{u}_j^k, \boldsymbol{x}_{\mathcal{N}_j}^k))^\top \boldsymbol{\lambda}_j^k \right)^\top \delta \bar{\boldsymbol{x}}_i \,\mathrm{d}t.
\end{aligned} \tag{48}$$

Considering the neighbor-affine formulation of dynamics (1) and cost terms (4), the Gâteaux derivative further simplifies to

$$\begin{aligned}
&\delta J_j(\boldsymbol{x}_j^k, \boldsymbol{u}_j^k, \boldsymbol{x}_{\mathcal{N}_j}^k)(\delta \boldsymbol{x}_i) \\
&= \int_0^T \left(\partial_{\boldsymbol{x}_i} l_{ji}(\boldsymbol{x}_j^k, \boldsymbol{x}_i^k) + (\partial_{\boldsymbol{x}_i} \boldsymbol{f}_{ji}(\boldsymbol{x}_j^k, \boldsymbol{x}_i^k))^\top \boldsymbol{\lambda}_j^k \right)^\top \delta \boldsymbol{x}_i \,\mathrm{d}t.
\end{aligned} \tag{49}$$

If the agents are additionally coupled via controls in their dynamics, see (36), the Gâteaux derivative extends to

$$\begin{aligned}
&\delta J_j(\boldsymbol{x}_j^k, \boldsymbol{u}_j^k, \boldsymbol{x}_{\mathcal{N}_j}^k, \boldsymbol{u}_{\mathcal{N}_j}^k)(\delta \boldsymbol{x}_i, \delta \boldsymbol{u}_i) \\
&= \int_0^T \left(\partial_{\boldsymbol{x}_i} l_{ji}(\boldsymbol{x}_j^k, \boldsymbol{x}_i^k) + (\partial_{\boldsymbol{x}_i} \boldsymbol{f}_{ji}(\boldsymbol{x}_j^k, \boldsymbol{x}_i^k))^\top \boldsymbol{\lambda}_j^k \right)^\top \delta \boldsymbol{x}_i \\
&\quad + (\boldsymbol{\lambda}_j^{k-1})^\top \boldsymbol{B}_{ji}(\boldsymbol{x}_j^{k-1})\, \delta \boldsymbol{u}_i \,\mathrm{d}t.
\end{aligned} \tag{50}$$

In Section II, the sensitivities are calculated recursively for the already augmented OCP (5). Recalling the definition of $\delta \boldsymbol{x}_i = \boldsymbol{x}_i - \boldsymbol{x}_i^k$, it is clear that (49) is linear w.r.t. $\boldsymbol{x}_i$ and can be incorporated as a linear term into the local cost function term $l_{ii}(\boldsymbol{x}_i)$ in (4). Thus, a repeated application of $\delta J_j(\boldsymbol{x}_j^k, \boldsymbol{u}_j^k, \boldsymbol{x}_{\mathcal{N}_j}^k)(\delta \boldsymbol{x}_i)$ still results in (49) and thus (9), i.e.,

$$\begin{aligned}
&\delta \bar{J}_j(\boldsymbol{x}_j^k, \boldsymbol{u}_j^k, \boldsymbol{x}_{\mathcal{N}_j}^k)(\delta \boldsymbol{x}_i) \\
&= \int_0^T \left(\partial_{\boldsymbol{x}_i} l_{ji}(\boldsymbol{x}_j^k, \boldsymbol{x}_i^k) + (\partial_{\boldsymbol{x}_i} \boldsymbol{f}_{ji}(\boldsymbol{x}_j^k, \boldsymbol{x}_i^k))^\top \boldsymbol{\lambda}_j^k \right)^\top \delta \boldsymbol{x}_i \,\mathrm{d}t.
\end{aligned} \tag{51}$$

This is also valid for the sensitivity w.r.t. $\boldsymbol{u}_i$. However, the calculation of the adjoint state in (6b) changes.

Appendix B
Additional Bounds

This section states auxiliary results that are needed in the convergence proofs of Theorem 2 and 3. The norm $\|\boldsymbol{x}_i^{r|k} - \boldsymbol{x}_i^{1|k}\|_{L_\infty}$ in (25) and (27) can be bounded for $r \geq 2$ as

$$\begin{aligned}
&\|\boldsymbol{x}_i^{r|k} - \boldsymbol{x}_i^{1|k}\|_{L_\infty} = \|\boldsymbol{x}_i^{r|k} - \boldsymbol{x}_i^{r-1|k} + \boldsymbol{x}_i^{r-1|k} + \cdots - \boldsymbol{x}_i^{1|k}\|_{L_\infty} \\
&\leq \|\boldsymbol{x}_i^{r|k} - \boldsymbol{x}_i^{r-1|k}\|_{L_\infty} + \cdots + \|\boldsymbol{x}_i^{2|k} - \boldsymbol{x}_i^{1|k}\|_{L_\infty} \\
&\leq p^{r-2}\|\boldsymbol{x}_i^{2|k} - \boldsymbol{x}_i^{1|k}\|_{L_\infty} + \cdots + \|\boldsymbol{x}_i^{2|k} - \boldsymbol{x}_i^{1|k}\|_{L_\infty} \\
&= \left(\sum_{j=0}^{r-2} p^j \right) \|\boldsymbol{x}_i^{2|k} - \boldsymbol{x}_i^{1|k}\|_{L_\infty} \leq \frac{1 - p^{r-1}}{1 - p} \|\boldsymbol{x}_i^{2|k} - \boldsymbol{x}_i^{1|k}\|_{L_\infty} \\
&\leq L_1 \frac{1 - p^{r-1}}{1 - p} \|\boldsymbol{\lambda}_j^{1|k} - \boldsymbol{\lambda}_j^{0|k}\|_{L_\infty} = L_1 \frac{1 - p^{r-1}}{1 - p} \|\Delta \boldsymbol{\lambda}_j^{k-1}\|_{L_\infty}
\end{aligned} \tag{52}$$

where (15a) was used for the second inequality and (21a) for the last inequality. Furthermore, it is exploited that the finite geometric series $\sum_{j=0}^{r-1} ap^j = a\frac{1-p^r}{1-p}$ has a closed-form solution [25]. Similarly, the norm $\|\boldsymbol{\lambda}_i^{r|k} - \boldsymbol{\lambda}_i^{1|k}\|_{L_\infty}$ in (25) and (27) can be bounded for $r \geq 2$ as

$$\begin{aligned}
&\|\boldsymbol{\lambda}_i^{r|k} - \boldsymbol{\lambda}_i^{1|k}\|_{L_\infty} = \|\boldsymbol{\lambda}_i^{r|k} - \boldsymbol{\lambda}_i^{r-1|k} + \boldsymbol{\lambda}_i^{r-1|k} + \cdots - \boldsymbol{\lambda}_i^{1|k}\|_{L_\infty}\\
&\leq \|\boldsymbol{\lambda}_i^{r|k} - \boldsymbol{\lambda}_i^{r-1|k}\|_{L_\infty} + \cdots + \|\boldsymbol{\lambda}_i^{2|k} - \boldsymbol{\lambda}_i^{1|k}\|_{L_\infty}\\
&\leq p^{r-1}\|\boldsymbol{\lambda}_i^{1|k} - \boldsymbol{\lambda}_i^{0|k}\|_{L_\infty} + \cdots + p\|\boldsymbol{\lambda}_i^{1|k} - \boldsymbol{\lambda}_i^{0|k}\|_{L_\infty}\\
&= p\left(\sum_{j=0}^{r-2} p^j\right)\|\boldsymbol{\lambda}_i^{1|k} - \boldsymbol{\lambda}_i^{0|k}\|_{L_\infty} \leq \frac{p-p^r}{1-p}\|\Delta\boldsymbol{\lambda}_j^{k-1}\|_{L_\infty}
\end{aligned} \tag{53}$$

with (15b) being used for the second inequality.

In the following, it is shown that $\|\Delta \boldsymbol{x}_i^k\|_{L_\infty} \to 0$ and $\|\Delta\boldsymbol{\lambda}_i^k\|_{L_\infty} \to 0$ for $k \to \infty$ imply that $\|\boldsymbol{x}_i^{r|k+1} - \boldsymbol{x}_i^{r|k}\|_{L_\infty} \to 0$ and $\|\boldsymbol{\lambda}_i^{r|k+1} - \boldsymbol{\lambda}_i^{r|k}\|_{L_\infty} \to 0$ as well. Given $\|\Delta \boldsymbol{x}_i^k\|_{L_\infty} \to 0$ and $\|\Delta\boldsymbol{\lambda}_i^k\|_{L_\infty} \to 0$, we get

$$\begin{aligned}
&\|\boldsymbol{x}_i^{r|k+1} - \boldsymbol{x}_i^{r|k}\|_{L_\infty} = \|\boldsymbol{x}_i^{r|k+1} - \boldsymbol{x}_i^{1|k+1} + \boldsymbol{x}_i^{1|k+1} - \boldsymbol{x}_i^{r|k}\|_{L_\infty}\\
&\leq \|\boldsymbol{x}_i^{r|k+1} - \boldsymbol{x}_i^{1|k+1}\|_{L_\infty} + \|\Delta\boldsymbol{x}_i^k\|_{L_\infty}\\
&\leq \|\boldsymbol{x}_i^{r|k+1} - \boldsymbol{x}_i^{1|k+1}\|_{L_\infty} \leq \frac{1-p^{r-1}}{1-p}\|\boldsymbol{x}_i^{2|k} - \boldsymbol{x}_i^{1|k}\|_{L_\infty}\\
&\leq L_1\frac{1-p^{r-1}}{1-p}\|\boldsymbol{\lambda}_i^{1|k} - \boldsymbol{\lambda}_i^{0|k}\|_{L_\infty} = \|\Delta\boldsymbol{\lambda}_i^k\|_{L_\infty} \to 0
\end{aligned} \tag{54}$$

where $\|\Delta \boldsymbol{x}_i^k\|_{L_\infty} \to 0$ is used in the second inequality and (52) is used for the third and fourth inequality. Similarly, we have

$$\begin{aligned}
&\|\boldsymbol{\lambda}_i^{r|k+1} - \boldsymbol{\lambda}_i^{r|k}\|_{L_\infty} = \|\boldsymbol{\lambda}_i^{r|k+1} - \boldsymbol{\lambda}_i^{1|k+1} + \boldsymbol{\lambda}_i^{1|k+1} - \boldsymbol{\lambda}_i^{r|k}\|_{L_\infty}\\
&\leq \|\boldsymbol{\lambda}_i^{r|k+1} - \boldsymbol{\lambda}_i^{1|k+1}\|_{L_\infty} + \|\Delta\boldsymbol{\lambda}_i^k\|_{L_\infty}\\
&\leq \|\boldsymbol{\lambda}_i^{r|k+1} - \boldsymbol{\lambda}_i^{1|k+1}\|_{L_\infty} \leq \frac{p-p^r}{1-p}\|\Delta\boldsymbol{\lambda}_j^k\|_{L_\infty} \to 0
\end{aligned} \tag{55}$$

where $\|\Delta\boldsymbol{\lambda}_i^k\|_{L_\infty} \to 0$ was used in the second inequality and (53) in the last inequality.

References

[1] R. Negenborn and J. Maestre, "Distributed model predictive control: An overview and roadmap of future research opportunities," *IEEE Control Syst. Mag.*, vol. 34, no. 4, pp. 87–97, Aug. 2014.

[2] M. A. Müller and F. Allgöwer, "Economic and distributed model predictive control: Recent developments in optimization-based control," *SICE J. Control, Meas., System Integration*, vol. 10, no. 2, pp. 39–52, 2017.

[3] L. Grüne and J. Pannek, *Nonlinear Model Predictive Control: Theory and Algorithms*. Cham, Switzerland: Springer, 2011.

[4] L. Grüne and K. Worthmann, "A distributed NMPC scheme without stabilizing terminal constraints," in *Distrib. Decis. Mak. Control*, London, U.K.: Springer, 2012, pp. 261–287.

[5] E. Franco, L. Magni, T. Parisini, M. M. Polycarpou, and D. M. Raimondo, "Cooperative constrained control of distributed agents with nonlinear dynamics and delayed information exchange: A stabilizing receding-horizon approach," *IEEE Trans. Autom. Control*, vol. 53, no. 1, pp. 324–338, Feb. 2008.

[6] W. B. Dunbar, "Distributed receding horizon control of dynamically coupled nonlinear systems," *IEEE Trans. Autom. Control*, vol. 52, no. 7, pp. 1249–1263, Jul. 2007.

[7] D. Burk, A. Völz, and K. Graichen, "A modular framework for distributed model predictive control of nonlinear continuous-time systems (GRAMPC-D)," *Optim. Engin.*, vol. 23, pp. 771–795, 2021.

[8] G. Stomberg, A. Engelmann, and T. Faulwasser, "A compendium of optimization algorithms for distributed linear-quadratic MPC," *at-Automatisierungstechnik*, vol. 70, no. 4, pp. 317–330, 2022.

[9] H. Scheu and W. Marquardt, "Sensitivity-based coordination in distributed model predictive control," *J. Process Control*, vol. 21, no. 5, pp. 715–728, 2011.

[10] T. Darure, V. Puig, J. Yamé, F. Hamelin, and Y. Wang, "Distributed model predictive control applied to a VAV based HVAC system based on sensitivity analysis," in *Proc. IFAC NMPC*, 2018, pp. 259–264.

[11] I. Alvarado et al., "A comparative analysis of distributed MPC techniques applied to the HD-MPC four-tank benchmark," *J. Process Control*, vol. 21, no. 5, pp. 800–815, 2011.

[12] H. Huber and K. Graichen, "A sensitivity-based distributed model predictive control algorithm for nonlinear continuous-time systems," in *Proc. IEEE Conf. Control Technol. Appl.*, San Diego, CA, USA, 2021, pp. 195–201.

[13] H. Scheu, J. Busch, and W. Marquardt, "Nonlinear distributed dynamic optimization based on first order sensitivities," in *Proc. IEEE Amer. Control Conf.*, Baltimore, MD, USA, 2010, pp. 1574–1579.

[14] M. Pierer von Esch, A. Völz, and K. Graichen, "Sensitivity-based distributed model predictive control: Synchronous and asynchronous execution compared to ADMM," *at-Automatisierungstechnik*, vol. 72, no. 2, pp. 91–106, 2024.

[15] H. Huber, D. Burk, and K. Graichen, "Comparison of sensitivity-based and ADMM-based DMPC applied to building automation," in *Proc. IEEE Conf. Control Technol. Appl.*, Trieste, Italy, 2022, pp. 546–553.

[16] K. Graichen, "A fixed-point iteration scheme for real-time model predictive control," *Automatica*, vol. 48, no. 7, pp. 1300–1305, 2012.

[17] K. Graichen and B. Käpernick, "A real-time gradient method for nonlinear model predictive control," in *Front. Model Predictive Control*, 1st ed., T. Zheng, Ed., Rijeka, Croatia: IntechOpen, 2012, pp. 9–28.

[18] J. Lunze, *Networked Control of Multi-Agent Systems*, 2nd ed., Bookmundo Direct, 2022.

[19] K. Graichen, "Nonlinear MPC with fixed-point iterations: Numerical and experimental validation," in *Proc. IFAC CAO*, Germany, 2015, pp. 62–67.

[20] P. D. Christofides, R. Scattolini, D. M. De La Pena, and J. Liu, "Distributed model predictive control: A tutorial review and future research directions," *Comput. Chem. Eng.*, vol. 51, pp. 21–41, 2013.

[21] J. Liu, D. Muñoz de la Peña, and P. D. Christofides, "Distributed model predictive control of nonlinear process systems," *AIChE J.*, vol. 55, no. 5, pp. 1171–1184, 2009.

[22] D. L. Debeljković and S. Stojanović, "The stability of linear discrete time delay systems in the sense of Lyapunov: An overview," *Sci. Tech. Rev.*, vol. 60, no. 3, pp. 67–81, 2010.

[23] S. Rajamani and S. Rajasekar, "Variation of response amplitude in parametrically driven single Duffing oscillator and unidirectionally coupled Duffing oscillators," *J. Appl. Nonlinear Dyn.*, vol. 6, no. 1, pp. 121–129, 2017.

[24] M. D. Mesarovic, D. Macko, and Y. Takahara, *Theory of Hierarchical Multilevel Systems*. New York, NY, USA: Academic Press, 2000.

[25] M. Abramowitz and I. A. Stegun, *Handbook of Mathematical Functions With Formulas, Graphs, and Mathematical Tables*, vol. 55. New York, NY, USA: Dover Publications, 1968.